# Supporting Information

## Mayeuf-Louchart et al. 10.1073/pnas.1407606111

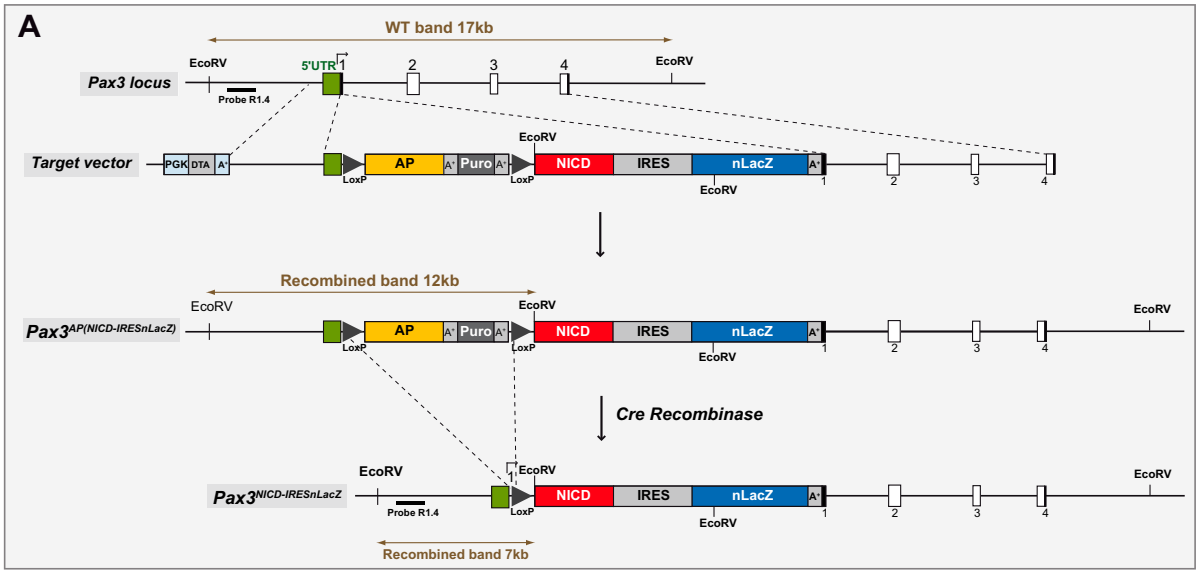


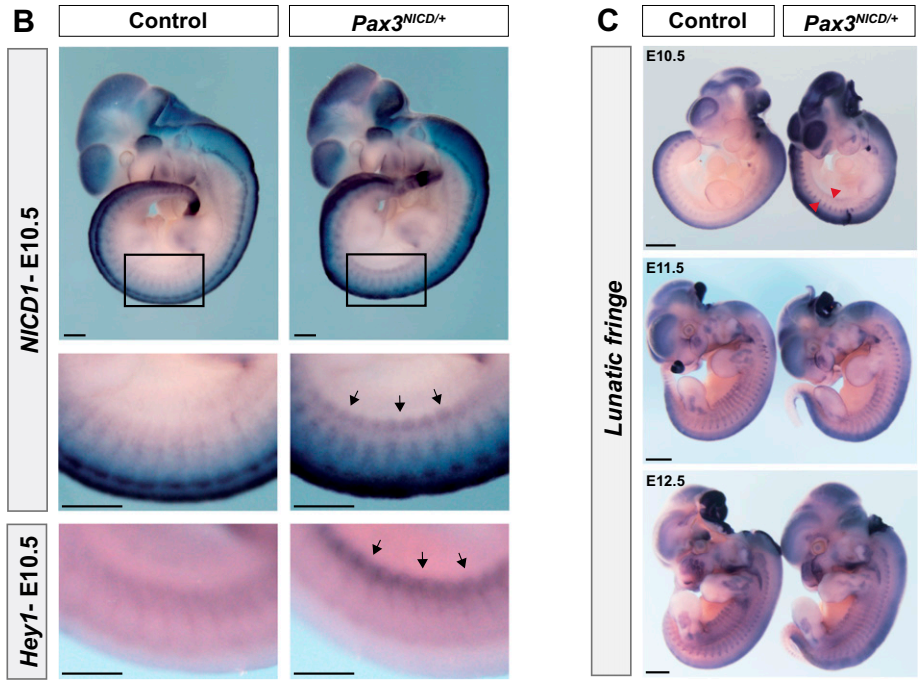


**Fig. S1.** Schema for generation of the *Pax3*$^{NICD}$ allele and validation of Notch gain-of-function. (*A*) The targeting construct contained 2.4 kb and 4 kb, respectively, of 5′ and 3′ genomic sequences from the first exon of *Pax3* surrounding an *Alkaline Phosphatase* (*AP*) reporter gene and a sequence *puromycin-pA* (*PuroA*), encoding the puromycin selection marker, flanked by *LoxP* sites, followed by a di-cistronic cassette containing a cDNA for the murine Notch intracellular domain (NICD) and an *IRESnLacZpA* reporter (IRES, internal ribosome entry site). A counter-selection cassette encoding the A subunit of diphtheria toxin (DTA) was inserted at the 5′ end of the vector. After homologous recombination in embryonic stem cells, *NICD-IRESnLacZ* expression from the *Pax3*$^{\Delta AP(NICD- IRESnLacZ)/+}$ allele is blocked by the floxed *AP-FRT-puromycin-pA* cassette. Crossing the mice generated from these cells with *Cre recombinase*-expressing mice generates the *Pax3*$^{NICD\text{-}IRESnLacZ}$ allele (*Pax3*$^{NICD}$). Probes (–) and restriction fragments (↔) are indicated, together with restriction enzyme sites. Rectangles (□) indicate *Pax3* exons. WT, wild type. (*B*) Whole-mount in situ hybridization for *NICD1* and *Hey1* in *Pax3*$^{NICD/+}$and control (*Pax3*$^{+/+}$) embryos, at embryonic day (E) 10.5 (Scale bar, 1 mm). (*Lower*) Close ups of the interlimb region (Scale bar, 1 mm). Arrowheads indicate up-regulation in the hypaxial somite where *Pax3* is strongly expressed between E9.5 and E11.5. (*C*) Whole-mount in situ hybridization for transcripts of *Lunatic fringe*, between E9.5 and E12.5, in *Pax3*$^{NICD/+}$ and control (*Pax3*$^{+/+}$) embryos. Red arrowheads point to up-regulation in the hypaxial and epaxial somite at E10.5 (Scale bar, 2 mm).

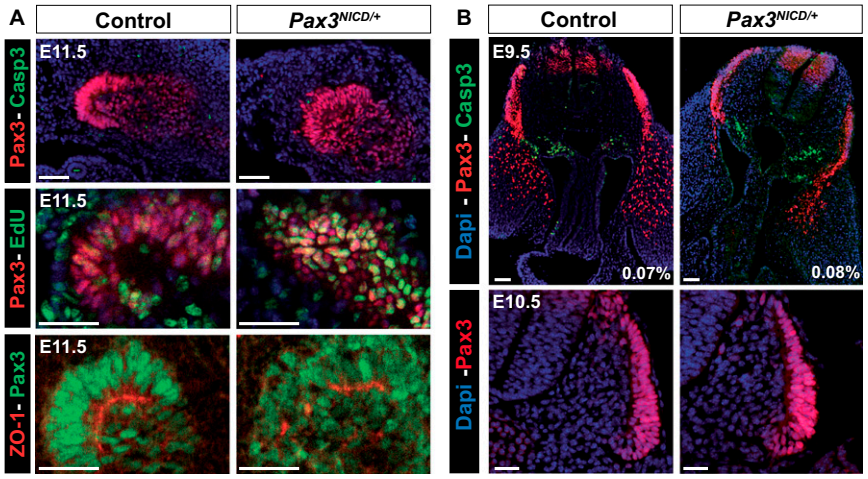


**Fig. S2.** Hypaxial defects in *Pax3*$^{NICD/+}$ embryos. (*A*) Transverse sections of trunk somites showing the hypaxial dermomyotome from control (*Pax3*$^{+/+}$) and *Pax3*$^{NICD/+}$ embryos at E11.5, after coimmunohistochemistry with antibodies for Pax3 and cleaved Caspase 3, that detects apoptosis (*Top*); EdU that—after pulse labeling—marks proliferating cells (*Middle*); and ZO-1, which marks basal epithelial cell polarity (*Bottom*) (Scale bar, 50 μm). (*B*) Immunohistochemistry on sections of control (*Pax3*$^{+/+}$) and *Pax3*$^{NICD/+}$ embryos, at forelimb level, with antibodies to Pax3 (red) and cleaved Caspase 3 (green) at E9.5 (*Upper*). Quantification of the percentage of Pax3$^{+}$ cells labeled with cleaved Caspase 3 is indicated at the bottom right of the panels ($P > 0.5$; $n = 10$ sections, 3 embryos). More migrating Pax3$^{+}$ cells are seen in the control. (*Lower*) Antibodies to Pax3 alone on a trunk somite at E10.5, where the hypaxial dermomyotome is intact (Scale bar, 100 μm).

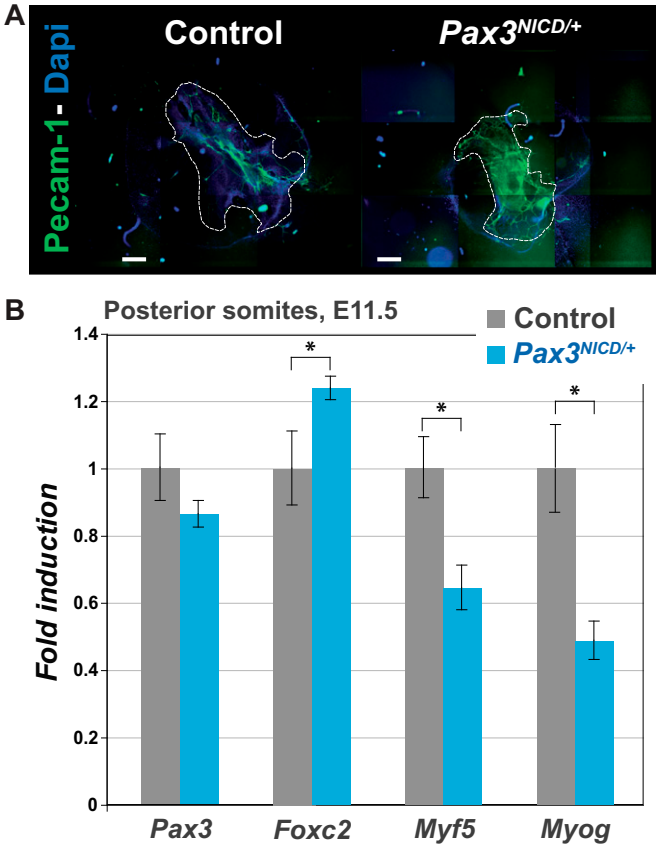


**Fig. S3.** Vascular versus myogenic fate in the caudal region of the embryo. (*A*) Immunohistochemistry with a Pecam-1 antibody on somite explants from *Pax3*$^{NICD/+}$ embryos compared with controls (Scale bar, 500 μm). (*B*) Quantitative RT-PCR analysis of transcripts for *Pax3*, *Foxc2*, *Myf5*, and *Myog* compared with *gapdh* on somites posterior to the hindlimb of *Pax3*$^{NICD/+}$ embryos at E11.5, compared with the controls (*Pax3*$^{+/+}$) taken as 1. *$P < 0.05$, error bars indicate SEM ($n = 3$ embryos).

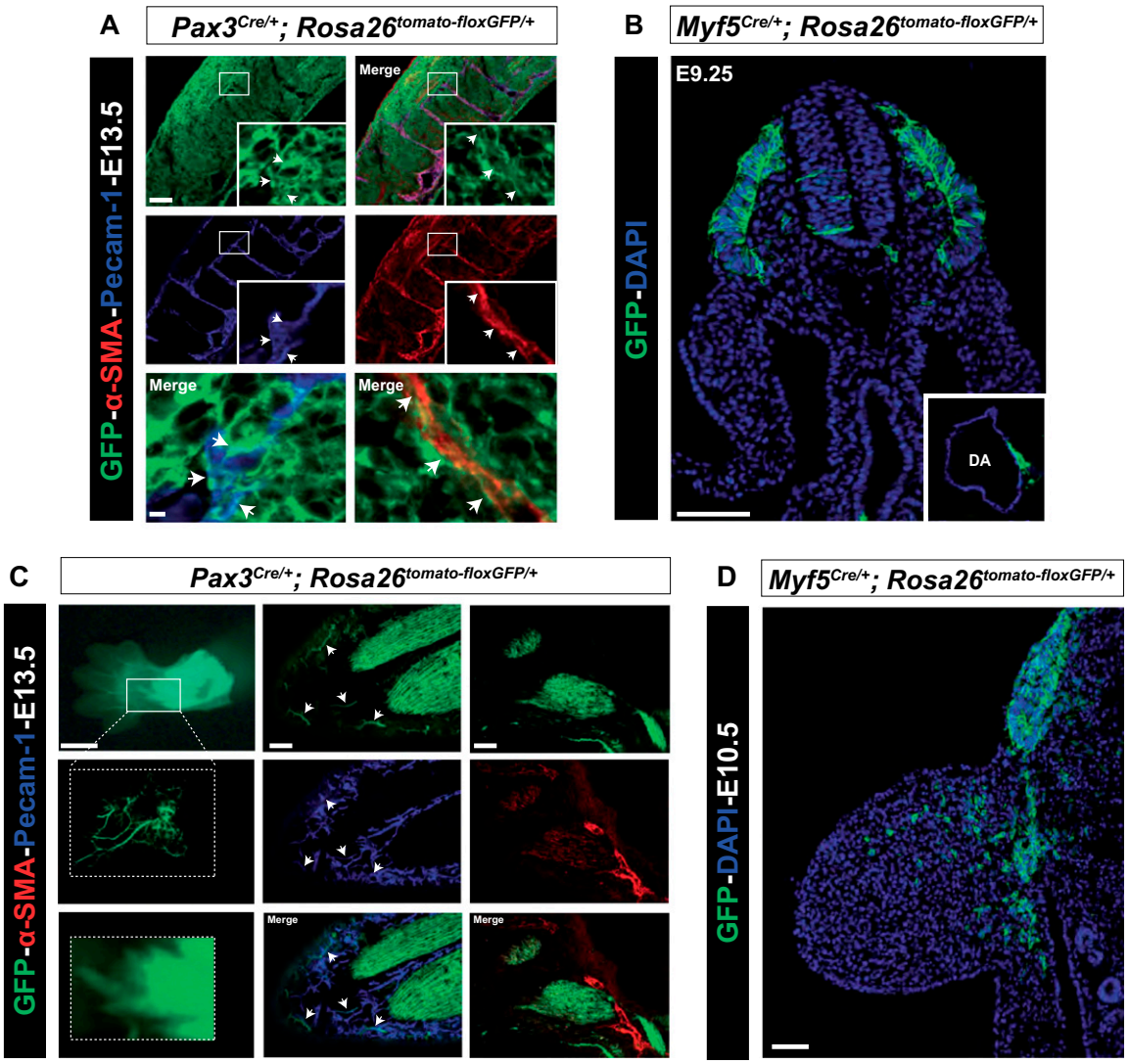


**Fig. S4.** Contribution of the somite to the endothelial and smooth muscle cells of the aorta and forelimbs. (*A*) Immunohistochemistry with Pecam-1 (blue), α-smooth muscle actin (α-SMA, red), and GFP (green) antibodies on sections of *Pax3*$^{Cre/+}$;*Rosa26*$^{tomato\text{-}floxGFP/+}$ embryos, at E13.5, in the caudal region (Scale bar, 100 μm). In the merged images (*Bottom*), colabeling is observed, as shown in enlargements of the boxed area shown on the left for Pecam-1 and GFP, (turquoise in merge) (*Bottom Right*) and on the right for α-SMA and GFP (yellow in merge) (*Bottom Left*) (Scale bar, 10 μm). White arrows indicate endothelial cells or smooth muscle cells derived from Pax3$^{+}$ somitic cells. (*B*) Immunohistochemistry on DAPI-stained sections of *Myf5*$^{Cre/+}$;*Rosa26*$^{tomato\text{-}floxGFP/+}$, at E9.25 (*Left*) (Scale bar, 100 μm), with GFP antibodies, in the trunk region at the level of the dorsal aorta (DA), shown in the lower right. (*C*) Immunohistochemistry on the forelimbs of *Pax3*$^{Cre/+}$;*Rosa26*$^{tomato\text{-}floxGFP/+}$ embryos at E13.5. (*Left*) GFP fluorescence on a forelimb (*Top*) and enlargements of the boxed region show superficial blood vessels (*Middle*) and muscle masses deeper in the tissue (*Bottom*) (Scale bar, 1 mm). The central panels show sections with an antibody to GFP (*Top*) and to the endothelial cell marker Pecam-1 (*Middle*). A merged image is shown in the *Bottom*. White arrows indicate somite derived (GFP$^{+}$) endothelial cells in blood vessels. (*Right*) Labeling, with antibodies to GFP and α-SMA (*Middle*) and a merged image (*Bottom*). In this case no colabeling is seen (Scale bar, 100 μm). (*D*) Immunohistochemistry on DAPI-stained sections of *Myf5*$^{Cre/+}$;*Rosa26*$^{tomato\text{-}floxGFP/+}$ embryos at E10.5, with the GFP antibody. GFP$^{+}$ cells are localized in the somite and in migrating cells in the limb (Scale bar, 100 μm).

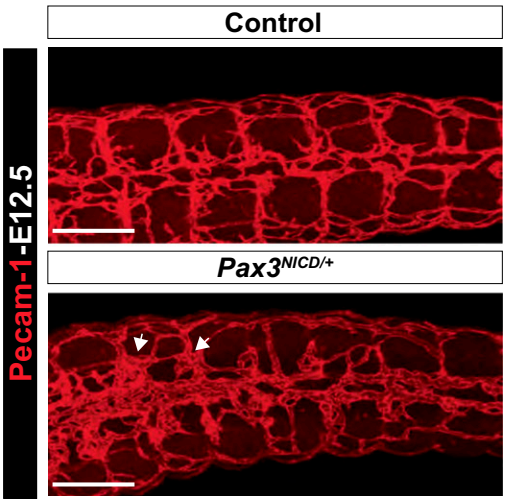


**Fig. S5.** Vessel disorganization in *Pax3*$^{NICD/+}$ embryos. Confocal pictures of whole-mount immunohistochemistry with a Pecam-1 antibody of the posterior region (tail level) of control (*Pax3*$^{+/+}$) and *Pax3*$^{NICD/+}$ embryos, at E12.5. White arrowheads indicate excess endothelial cells associated with and around vessels, in *Pax3*$^{NICD/+}$ embryos (Scale bar, 200 μm).

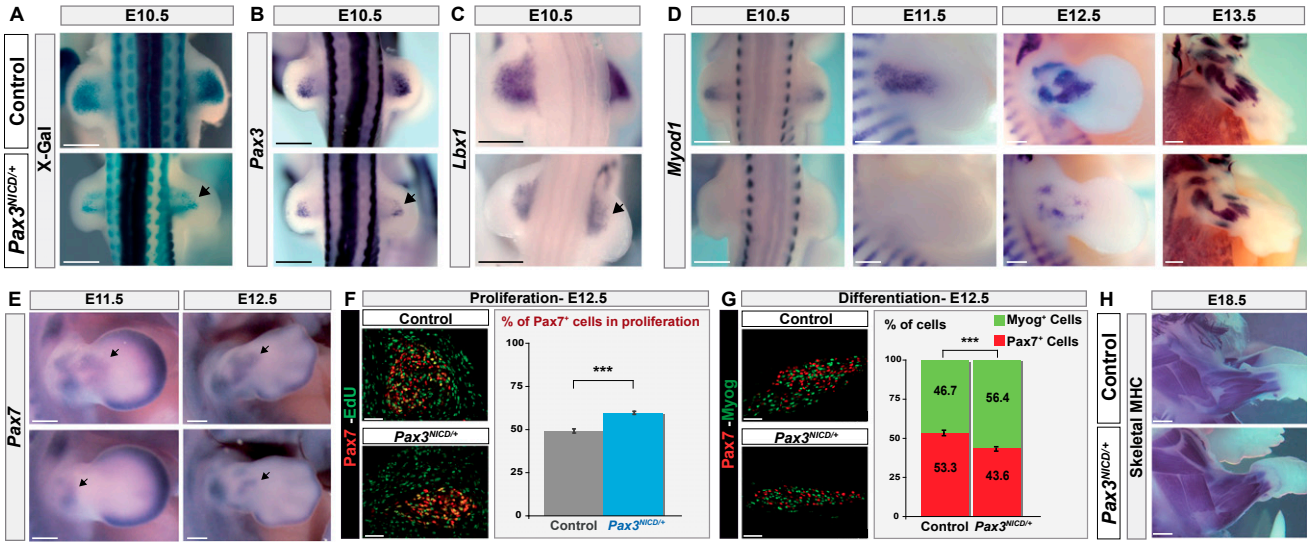


**Fig. S6.** Defects in myogenesis and later recovery in *Pax3*$^{NICD/+}$ embryos. Comparison of *Pax3*$^{NICD/+}$ and control (*Pax3*$^{+/+}$) embryos at the forelimb level. (*A*–*C*) Whole-mount X-Gal staining (*A*) and in situ hybridization for transcripts of *Pax3* (*B*) and *Lbx1* (*C*) in *Pax3*$^{NICD/+}$ and control embryos (*Pax3*$^{IRES\text{-}nLacZ/+}$ and *Pax3*$^{+/+}$, respectively), at the forelimb level at E10.5. Black arrows indicate a decrease in the number of X-Gal–labeled cells and of cells expressing *Lbx1* and *Pax3* transcripts in the forelimbs of *Pax3*$^{NICD/+}$ embryos. (*D*) Whole-mount in situ hybridization for transcripts of *Myod1* between E10.5 and E13.5. (*E*) Whole-mount in situ hybridization for transcripts of *Pax7* in forelimbs at E11.5 and E12.5. Arrows point to forming muscle masses (staining of the distal extremity is because of trapping of the probe) (*A*–*E* Scale bar, 2 mm). (*F*) Immunohistochemistry on sections of forelimbs at E12.5, with a Pax7 (red) antibody and EdU (green) staining of proliferating cells, in *Pax3*$^{NICD/+}$ and control (*Pax3*$^{+/+}$ ) embryos. Quantification of the percentage of Pax7$^{+}$ cells that are also EdU$^{+}$. ***$P < 0.001$, error bars indicate SEM ($n = 100$ limb bud sections). (*G*) Immunohistochemistry on sections of forelimbs with Pax7 (red) and Myogenin (Myog) (green) antibodies, at E12.5, in *Pax3*$^{NICD/+}$ and control (*Pax3*$^{+/+}$ ) embryos. Quantification of the percentage of differentiating cells (Myog$^{+}$) compared with progenitor cells (Pax7$^{+}$), ***$P <$ 0.001, error bars indicate SEM ($n = 20$ limb bud sections) (*F* and *G* Scale bar, 50 μm). (*H*) Whole-mount immunohistochemistry with a Fast Skeletal myosin heavy chain (MHC) antibody, at E18.5, where skeletal muscle masses are labeled in purple (Scale bar, 1 mm).

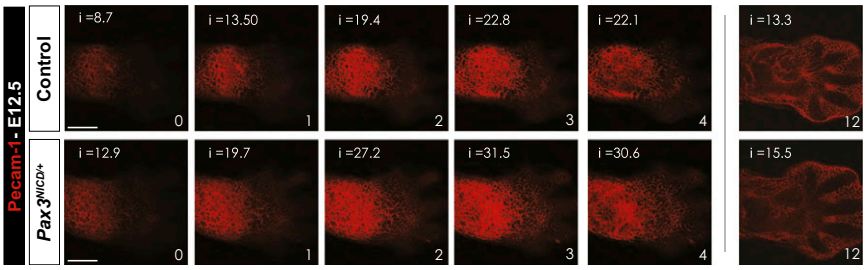


**Fig. S7.** Increase of endothelial cells in superficial vessels in limbs of *Pax3*$^{NICD/+}$ embryos. Whole-mount immunostaining with an antibody to Pecam-1 on the forelimbs of control (*Pax3*$^{+/+}$) and *Pax3*$^{NICD/+}$ embryos, at E12.5. Pictures represent the 3D projection (mean value) of the images obtained with confocal sectioning of the limb buds. Scanning of confocal sections of forelimbs was carried out from the surface (0) to the interior (12). Signal intensity (i) was automatically measured for the image of each section. Similar results were seen with a ventral to interior series of sections (Scale bar, 500 μm).

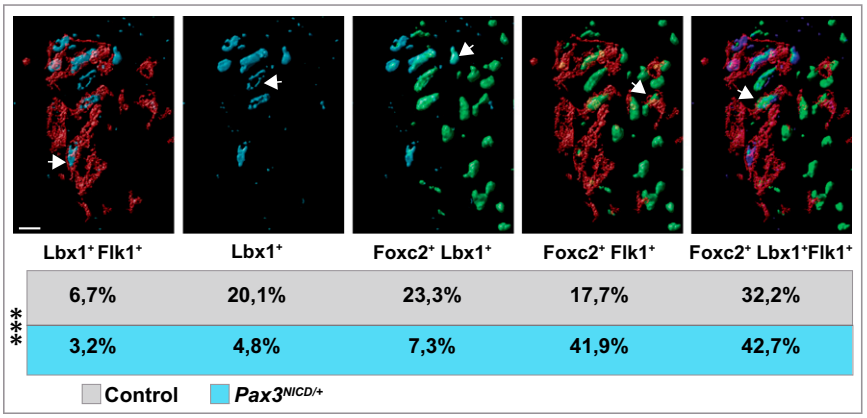


**Fig. S8.** Repartition of cells in the hypaxial somite region at E9.25. Three-dimensional representation (Huygens software) of immunohistochemistry with Lbx1 (blue), Flk1 (red), and Foxc2 (green) antibodies in the hypaxial region of *Pax3*$^{NICD/+}$ embryos at E9.25 (*Upper*) (Scale bar, 10 μm). Quantification of the proportion of each category of cells (white arrows) in control (*Pax3*$^{+/+}$) and *Pax3*$^{NICD/+}$ embryos (*Lower*). ***$P < 0.001$, error bars indicate SEM ($n > 16$ limb bud sections).

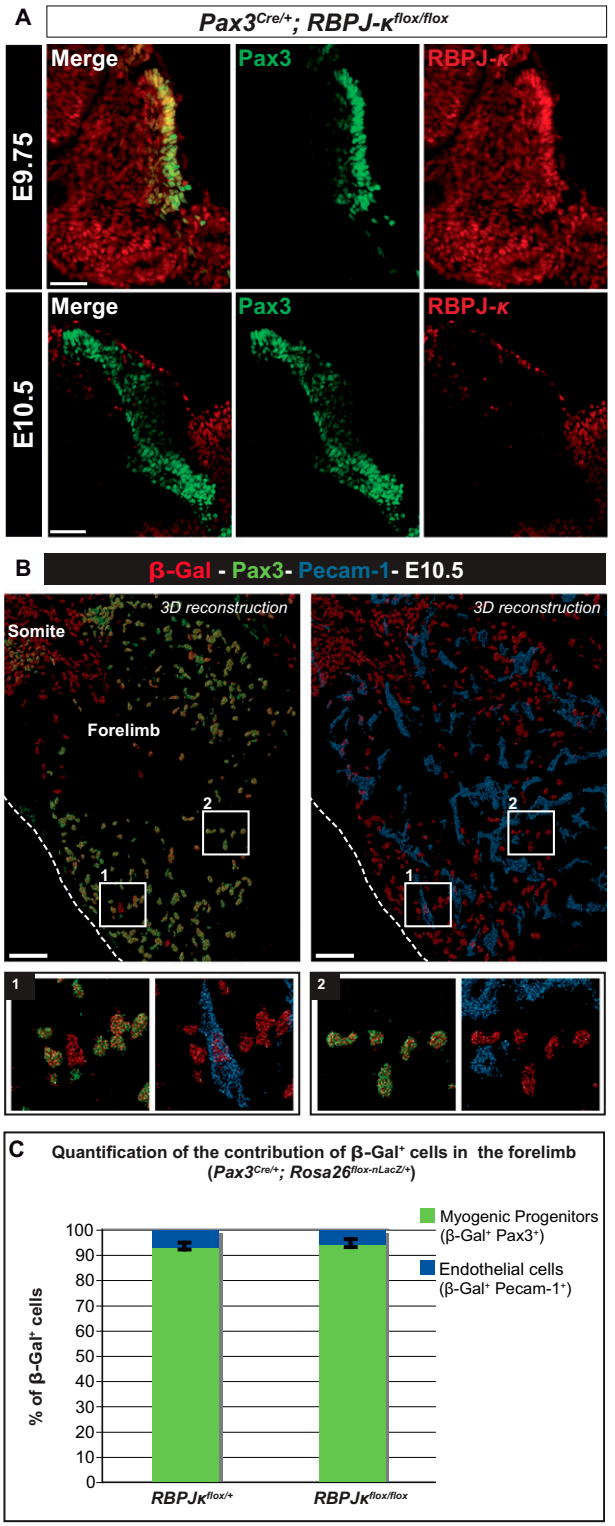


**Fig. S9.** Conditional loss-of-function for RBPJ-κ in Pax3$^+$ cells. (*A*) Transverse sections of trunk somites, at the forelimb level, from *Pax3*$^{Cre/+}$;*RBPJ-κ*$^{flox/flox}$ embryos at E9.75 and E10.5, after coimmunohistochemistry with antibodies for Pax3 and RBPJ-κ, show that the RBPJ-κ protein is still present at E9.75 in loss of function embryos and is absent at E10.5 (Scale bar, 50 μm). (*B*) Three dimensional representation (Huygens software) of immunohistochemistry with β-Galactosidase (β-Gal) (red), Pax3 (green), and Pecam-1 (blue) antibodies, at E10.5, in the forelimb of *Pax3*$^{Cre/+}$;*RBPJ-κ*$^{flox/+}$;*Rosa26*$^{flox\text{-}nLacZ/+}$ and *Pax3*$^{Cre/+}$;*RBPJ-κ*$^{flox/flox}$;*Rosa26*$^{flox\text{-}nLacZ/+}$ embryos. "1" and "2" represent enlargements of the boxed areas in *B* (Scale bar, 50 μm). (*C*) Quantification of the percentage of endothelial cells derived from the somite (β-Gal$^+$ Pecam-1$^+$) and myogenic progenitor cells (β-Gal$^+$ Pecam-1$^+$). $P > 0.5$, error bars indicate SEM ($n = 3$ embryos).

## Other Supporting Information Files

*SI Methods* (DOC)